TORQUE RIPPLE MINIMIZATION OF BRUSHLESS DC MOTOR USING INTELLIGENT CONTROL TECHNIQUE

M.Vijayakumar

Department of Electrical and Electronics Engineering, K.S.R. College of Engineering, Tiruchengode,
Tamil Nadu, India,
vijayresearch24@gmail.com

P.S.Periasamy

Department of Electronics and Communication Engineering, K.S.R. College of Engineering, Tiruchengode,
Tamil Nadu, India

Abstract: *For improving the speed and torque of the BLDC motor is applied an improved method is based Direct Torque Control (DTC) technique. Gravitational Search Algorithm (GSA) and the Radial Basis Function Neural Network (RBFNN) method are equated in an improved method. By updating the randomized stricture, the updating performance of the GSA is showed. The RBFNN is used for developed the execution of the GSA and modernizing the stricture. The huge torque ripple in commutation part found once the DTC approach is worked in the conduction mode. FOPID is improved as the speed and torque control of BLDC motor. In conclusion, the proposed method is applied in the MATLAB/Simulink platform. The functional maximized of the suggested technique is recognized and combined with the modern strategies such as Genetic Algorithm (GA) and Particle Swarm Optimization (PSO)-RBFNN procedures.*
Keywords: BLDC motor, speed, torque, GSA, RBFNN, FOPID, GA, PSO and EMF

1.Introduction

Flywheel is conceived as the primary spacecraft attitude control actuator. The flywheel reaction momentum can alter the spacecraft axial position accurately associating suitable accelerated torque to the motor shaft. The major objective for the actuator control system is unambiguous response to the torque command. In industrial applications, the BLDC motor has collected widespread recognition [1]. High power density, large torque to inertia ratio, simplicity in their control compact forms, high efficiency, and also easy of control and low maintenance is the benefits of BLDC motors [2]. Low cost and high efficiency variable speed motor drives have developing interest throughout the years [4]. An precise and ripple-free instant torque is great place for the BLDC motor and Torque smoothness is required as high-performance motion control applications [5]. In current years, the torque ripple minimization and the control performance enhancement of the BLDC motor might have been selected. Commutation torque ripple, the torque ripple is formed by diode freewheeling of inactive phase, and the torque ripple is induced by the non-ideal back Electro Motive Force (EMF) are the major research works [6].

Production with BLDC motor control approaches is usually is established on the current and torque control methods. As reducing the torque ripples, a generalized harmonic injection to determine out optimal current waveforms [8]. The most general speed evaluation technique is established back EMF as BLDC motors. Operation rotor speeds evaluate the magnitude of the back EMF. The back EMF is not adequate to evaluate the speed and position since of inverter and parameter nonlinearities at low speeds [10]. The most gainful way is position sensor-less drive. Sensor-less position estimation of the BLDC motor is established on simple logic nothing like vector sensor-less controls of PMSM [12]. BLDC Motor drives alongside their applications admit the position sensors as Hall-impact, resolver, or supreme encoder for exact execution of current substitution in stator windings and additionally approval of reasonable wanted control. In any case, establishment of these sensors in the engine of the control will make the engine drive framework is determine a few issues [14].

For position detection, the motor torque constant is applied as a reference signal. To reach high accuracy estimation of the rotor position is applied as sliding-mode observer and Kalman filter methods. Cogging torque, the flux harmonics, the partial demagnetization of the permanent magnets, errors in current or rotor position measurement, and phase unbalancing are different sources of torque pulsations in a PMSM [15]. An applying the hybrid technique, the speed and torque ripple is estimated. In the document, the suggested strategies are made cleared in the section 3. The recent research works are described in section 2. Here is the discussion of the results of the suggested technique is described in section 4. It fulfills the document in section 5.

2. Recent Research Works: An Overview

Numbers of research works have once subsisted in literature is derived from the torque and speed of BLDC motor. Certain works were assessed at this time.

A Finite Control Set-Model Predictive Control (FCS-MPC), the fault-tolerant control algorithm of a five-phase BLDC motor has been demonstrated by Mehdi Salehifar et al. [16]. A Fault Diagnosis (FD) technique is established on existing data from the control block was offered. This strategy was simple, robust to general transients in motor and skilled to localize multiple open circuit faults.

Some fault-tolerant control systems for BLDC motor drives have been analyzed by Lianghui Dong et al. [17]. The procedure is established on fault diagnosis and its classification, and successive signal reconstruction. The accessible fault-tolerant strategies could be simply and quickly understood as conventional drive systems, either by adding a simple auxiliary circuit or by adding the code in the existing driver in the Hall sensors and the driver.

A simple, cost effective and resourceful BLDC motor drive for Solar Photo Voltaic (SPV) array supplied water pumping system has been proposed by Rajan Kumar et al. [18]. A zeta converter was applied to extract the maximum power from the SPV array. An-Chen Lee et al. [19] have analyzed the current waveform through conducting phase error in commutation and non-ideal back-EMF. Although relation amongst the elapsed time of phase error in commutation with current waveform, the applied voltage then the non-ideal back-EMF was gained.Kun Xia et al. [13] have increased and inquired the cause of commutation torque ripple and a nonlinear transient model of the phase current in the commutation interval.

For the most part, PID controller is the important choice to control the speed of the BLDC machine. Particular technique for control can be needed with insightful framework depends on fluffy rationale and neural system approach is conquered the above issues. An applying the neural systems are prepared disconnected by means of information from traditional PI controller. It won't disseminate the productive powerful reaction. The consistent principles are developed however it necessitates the greater investment to perform or settle on the choice guidelines in the fluffy rationale controller. Be that as it may, most extreme time, fluffy rationale based controller conveys preferred outcomes over the regular and neural system. From the writing survey, the PI controller is the attractive speed controller for BLDC Motor, yet PI controller creates dormant reaction in the framework, and furthermore it

develops vulnerability issue specifically working states of the BLDC Motor. Just barely advancement calculation based PI controller is built up for controlling the speed and torque of the BLDC Motor as Genetic Algorithm (GA), Particle Swarm Optimization (PSO) calculation and Bat calculation and so forth. The GA task depends on hereditary administrators are irregular in nature then it induces infeasible arrangement with over the top computational time. A productive strategy based propelled PID controller is basic to tackle the above issues of BLDC Motor is applied to maintain a strategic distance from these deficiencies. In this original copy, a half and half procedure based torque swell minimization is expected for the BLDC Motor drive framework. The suggested swell minimization strategy of the BLDC Motor drive is approved by models and clarified in the segment 3.

3. Mathematical modeling of BLDC motor

A standard typical BLDC Motor drive with rotor position input is originate in Fig. 1(a). A diode rectifier is an expansive electrolytic capacitor with converter nourished through rotor position information in the BLDC Motor drive framework. The electrolytic capacitor is greater in size and weight, and its lifespan is halfway by the working temperature [11]. Like this, to lessen the expense, limit the level of the divided region and to build the resolute quality, a BLDC motor drive without a DC interface capacitor is portrayed in Fig. 1. The engine drive is worked specifically from a leveled mains supply without the DC connect capacitor. The expense of the usual engine drive is basically diminished because of the nonappearance of the DC interface capacitor to the burden of torque swells which are unpreventable and anticipated that connection with zero crossing points of the mains supply. The comparable model of the BLDC Motor drive structure with the likelihood of three-stage symmetric stator winding is established in Fig. 1
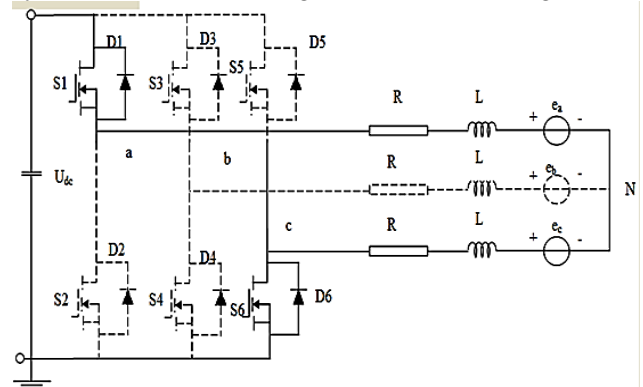
Fig.1: Equivalent model of the BLDC motor

The terminal voltage equation of three-phase stator windings is expressed as

$$\begin{bmatrix} u_a \\ u_b \\ u_c \end{bmatrix} = \begin{bmatrix} R & 0 & 0 \\ 0 & R & 0 \\ 0 & 0 & R \end{bmatrix} * \begin{bmatrix} i_a \\ i_b \\ i_c \end{bmatrix} + \begin{bmatrix} L & 0 & 0 \\ 0 & L & 0 \\ 0 & 0 & L \end{bmatrix} * \frac{d}{dt} \begin{bmatrix} i_a \\ i_b \\ i_c \end{bmatrix} + \begin{bmatrix} e_a \\ e_b \\ e_c \end{bmatrix} + u_N$$

(1)

From the above equation, R and L are referred as the stator resistance and inductance. Next u_a, u_b, u_c are stated as the terminal voltages of the three phase windings. The stator currents and phase back EMF are signified by i_a, i_b, i_c, e_a, e_b and e_c correspondingly. The neutral point of the motor voltage is referred as u_N. The electromagnetic torque is stated by

$$T_e = \frac{e_a i_a + e_b i_b + e_c i_c}{\omega_m}$$

(2)

Where, ω_m is indicated as the mechanical angular velocity of the rotor. BLDC motor normally operates in two-phase conduction mode which means only two windings are wired with the chosen rotor positions. Supposing that the current flows from phase-x winding to phase-y winding, and phase-z winding is inactive, $i_z = 0$, the current control model can be derived from (1) as

$$\frac{di_x}{dt} = -a i_x + b(u - e_{sy}) + f$$

(3)

Where, $a = \dfrac{R}{L}$ and $b = \dfrac{1}{2L}$ are computed. After that, the e_{xy} is evaluated by applying the following equation,

$$e_{xy} = e_x - e_y$$

(4)

From the above values, e_{xy} be the line-to-line back EMF, u be the average voltage amongst the two conducting phases in every control interval and f are the unstructured uncertainties are induced by sensors' dynamic, sampling noise, the inverter nonlinearity, or other high-frequency dynamic characteristics [17]. Similarly, the reference current can be gotten from (2) as,

$$i_x^* = \frac{T_e^* \omega_m}{e_{xy}}$$

(5)

Where, T_e^* be referred as the reference torque of the BLDC motor.

The torque swells are activated by non-perfect back EMF in the BLDC Motor. Pay of torque swells are aligning the controller and control calculation expands prevalence in spite of changing physical structure of the BLDC Motor with the mechanical enhancements. At that point to lessen the torque swells, a half and half method is crucial in the BLDC Motor drive framework. Next, the dc interface voltage, current and speed of BLDC Motor are assessed. Currently, the Gravitational Search Algorithm (GSA) and Radial Basis Function Neural Network (RBFNN) are built up as the execution of BLDC Motor. The detailed portrayal of the suggested approach with the BLDC Motor is clarified with the ensuing fragment.

3.1. Overview of BLDC motor with Proposed Hybrid Controller

The BLDC Motor drive framework is studied via suggested the half and half method in the section. The suggested half and half procedure is collecting of Gravitational Search Algorithm (GSA) and Radial Basis Function Neural Network (RBFNN). The torque and speed of the BLDC Motor is estimated dependent on the variety of torque. The aim of the proposed half and half system is the torque swell minimization. The torque and speed routine of the BLDC Motor is raised with the activity of proposed half and half technique to reach the goal work. Currently, the suggested half breed approach based BLDC Motor control structure is found in the figure 2. The point by point portrayal of the control structure is explained in the accompanying,
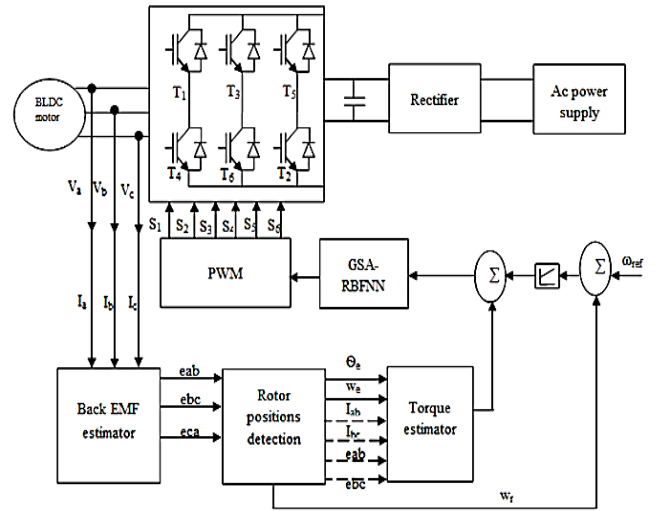
Fig. 2: Schematic diagram of GSA-RBFNN method-based BLDC motor

By and large, the BLDC Motor comprises two circles are the inward circle and the external circle. In the inward circle admits the DTC control framework and the external circle cover the speed control loop. Now, the external control circle is applied the FOPID controller for the BLDC Motor. The two circles are achieved the ideal task of BLDC

Motor. Similarly, the suggested control framework contains Voltage Source Inverter (VSI), exchanging gadget states, position discovery and speed computation, and electromagnetic torque estimation [9].

3.2. Control strategy of BLDC motor

The control strategy of BLDC motor is characterized five effective key blocks. The blocks are denoted as speed controller, estimators of the back-EMF, speed, and torque comparator, differentiating input voltage complementary controller consistently. These blocks are applied to reduce the torque-ripple at high-speed and switching logic i.e. determinant of the inverter switching status. The output of the suggested controller is used to get phase-to-phase back-EMFs evaluation for identifying rotor position and speed.

3.2.1. Enhanced FOPID controller with aid of GSA

Normally, the established Proportional-Integral-Derivative (PID) controller is applied for modern applications in light of its facility in acknowledgment and tuning. The rescheduling of subsidiary and incorporation arrange from number to partial request offers greater adaptability in structure of the controller hence controlling the extensive variety of elements of a framework. In partial request controller other than c proportional (k_p), Integral (k_i) and Derivative (k_d), the controller have integral order (λ), and the derivative order (μ), so the utilization of two additional administrators admits the two new levels of opportunity to the controller and creates it feasible to upgrading the execution for the expected PID controllers. Fragmentary request differential condition is applied to express the Fractional Order Proportional-Integral-Derivative (FOPID) controller ($P_i^{-\lambda}D^{\mu}$). The differential condition of fragmentary request controller is depicted as,

$$u(t) = k_p e(t) + k_i D_t^{-\lambda} e(t) + k_d D_t^{\mu} e(t) \qquad (6)$$

$$e(t) = \left(T^{actual} - T^{t \arg et}\right) \qquad (7)$$

      Where e (t) is the error signal and u (t) be the control signal.

      In PID controller design, this extension of integral and derivative order will specify much more flexibility and accuracy. Now, the input of FOPID controller is the error value of torque ($Te(t)$). The torque error is gotten from the difference amongst the actual value and the reference value. The error signal is reduced by applying the Gravitational Search Algorithm (GSA) to reach the objective function. Consequently, the

updated function of GSA is successfully applied as the input of RBFNN and it is well trained for developing the control pulses. Afterward, the suggested method approves to well forming the torque ripples minimization of BLDC motor. Allowing to regulated output, the PWM control signal is formed for regulating the inverter gate. Currently, a comprehensive analysis of the GSA and RBFNN based FOPID controller is reviewed in the following section.

3.2.2. Gravitational Search Algorithm

GSA is another headway calculation which has been mindfulness between the standard analysts as of late. The calculation is social occasion of searcher specialists that connection with one another by means of the gravity urges. The calculation is wanted to build the accomplished in the pursuit and misuse limits of a people based calculation in light of gravity standards. The situation of the mass addresses the arrangement of the issue where the gravitational and inertial masses are settled a wellbeing work. The calculation is sought by altering the gravitational and torpidity masses where as each mass demonstrates an answer. Masses are pulled in by the heaviest mass. At that point the heaviest mass shows a perfect approach in the request space [7]. Presently, the FOPID controller gain parameters are afforded to the contribution of the GSA and accomplished the relating yield. The methods for GSA as following:

Step 1: Randomized initialization
Initially, the FOPID controller parameters are started at random such as, K_p, K_i, K_d, λ and μ correspondingly. The initialized system parameters are considered as a function which referred as X_i. Similarly, the torque values are applied to estimate the objective function. The positions of the N number of agents are started systematically is verified in below equation,

$$X_i = \left(x_i^1, x_i^2, ...,x_i^d,.....x_i^D\right);$$
$$for, i = 1,2,.....,N; \ d = 1,2,3.......,D \qquad (8)$$

Where,

    D Corresponds to the element of mediator

    x_i^d Corresponds to the location of the ith mediator in the dth element

Step 2: Computation of the total force in diverse directions.
The Newton law of gravity, the gravitational force between two objects is directly proportional to the product of their masses and inversely proportional to the square of the distance amongst the objects.
In accordance with the gravitational law,

$$F_{ij}^{d}(t) = G(t) \times \left(\frac{M_{pi}(t) * M_{aj}(t)}{R_{ij}(t) + \varepsilon} \right) \times \left(x^{d}{}_{j}(t) - x^{d}{}_{i}(t) \right)$$

(9)

Where,

$M_{pi}(t)$ Corresponds to the submissive gravitational load combined to mediator

$M_{aj}(t)$ Corresponds to dynamic gravitational load combined to mediator

$G(t)$ Corresponds to the gravitational stable at time t

ε Corresponds to the miniature of the steady

The $R_{ij}(t)$ is the Euclidian expanse between two mediators i and j which is explained as,

$$R_{ij}(t) = \| X_{i}(t), X_{j}(t) \|_{2}$$

(10)

Step 3: Acceleration of agents' algorithm

To afford a stochastic attribute to our GSA algorithm, we presume that the whole drive that perform on middle person in a component be an unevenly stacked figuring of mechanical assembly of the powers are linked from previous arbiters which is declared as condition (13).

$$F_{i}^{d} = \sum_{j=1,\, j \neq 1}^{N} rand_{j} F_{ij}^{d}(t)$$

(11)

Where, $rand_{j}$ refers the arbitrary quantity in the period is $[0,1]$. Then the law of force is processed by the equation

$$a_{i}^{d}(t) = \frac{F_{i}^{d}(t)}{M_{ii}(t)}$$

(12)

Where, $M_{ii}(t)$ signifies the inertial load of ith mediator

Step 4: Computation of acceleration and velocity

Velocity and the position of the agents at successive iteration $(t+1)$ are computed is established on the following equations

$$v_{i}^{d}(t+1) = rand_{i} \times v_{i}^{d}(t) + a_{i}^{d}(t)$$

(13)

$$x_{i}^{d}(t+1) = x_{i}^{d}(t) + v_{i}^{d}(t+1)$$

(14)

Where, $rand_{j}$ relates to the identical arbitrary variable in the period $[0,1]$, then the working condition of the arbitrary amount is a randomized feature to the hunt. An established on the fitness function, the optimal results are found. The fitness function is assessed by the equations are displayed as follows.

$$fit(X_{i}) = \min(e(t))$$

(15)

From the primary fitness value, the least minimum fitness and the quality of best solutions are selected.
Step 5: Update G(t), best(t), worst(t) and Mi(t)for i= 1,2,...,N.

$$M_{ai} = M_{pi} = M_{ii} = M_{i} \; ; i = 1,2,3,......,N$$

(16)

$$m_{i}(t) = \frac{fit_{i}(t) - worst(t)}{best(t) - worst(t)}$$

(17)

$$M_{i}(t) = \frac{m_{i}(t)}{\sum_{j=1}^{N} m_{j}(t)}$$

(18)

Where, $fit_{i}(t)$ demonstrates the signifying fitness value of the mediator i at time t, and nastiest (t) and finest (t) are distinct as under,

$$best(t) = \min_{j \in \{1,2,3,.....N\}} fit_{j}(t)$$

(19)

$$worst(t) = \max_{j \in \{1,2,3,.....N\}} fit_{j}(t)$$

(20)

Step 6: Compute the gravitational constant

$$G(t) = G_{0} * \exp\left(-a * \frac{iter}{iter_{\max}} \right)$$

(21)

The output of the best FOPID parameters value is estimated in the above equality. In the updated process, the RBFNN is used for receiving the optimal results. The detailed process of the RBFNN is denoted in the next section.

3.2.3. Radial Basis Function Neural Network

NN is the non-typical information methodology for estimating the yield since its instructing and doesn't admit some scientific impersonation for its structure. The RBFNN is the kind of NN has three layers are input layer, shrouded layer, and yield layer. The hidden center points complete plan of extended commence work and the yield center points perform coordinate summation fills in as in MLP [3]. The RBFNN is applied to change the procedure of GSA. The count wellsprings of information are afforded to the commitment of the RBFNN which is established as. At that point the neurons are sharpened with the particular conditions drive at an exact goal. Currently, the back spread getting ready figuring is applied for organizing the neural framework. The readied framework is inquired with refit the GSA parameters. The information origins and yields are showed as the X1, X2 and Y reliably. In Fig.3, the structure of the framework is performed. The detail depiction of RBFNN is streamlined in the subsequent territory.
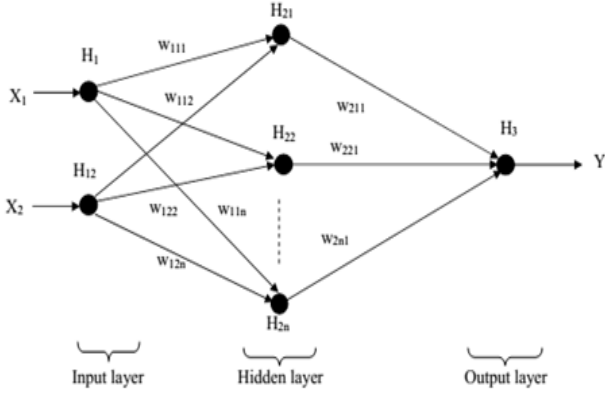
**Fig.3 Structure of proposed RBFNN technique
Steps for back propagation training algorithm**

1. To start the input layer, hidden and output layer weights of the neural network at random. Now, the input is denoted as $X_i = (x_1, x_2, \ldots \ldots x_n)$, which comprises the low frequency extracted signals of the induction motor. The neuron weights of the hidden layer & output layer are started in the specific interval $[w_{min}, w_{max}]$. The input layer to the hidden layer weights are depicted as $(w_{111}, w_{112}, \ldots w_{11n})$. Likewise, the hidden layers to the output layer weight are labeled as $(w_{211}, w_{212}, \ldots w_{2nk})$.

2. Learning the network along with the input and an equivalent target.

3. Assess the back-propagation error of the target (output) $Y_m = Y_1, Y_2, Y_3, Y_4$ are clarified by following,

$$BP_{Error}^m = (Y_m^{NN})_T - (Y_m^{NN})_{out} \qquad (22)$$

Where, $\left(Y_m^{NN}\right)_T$ be the network target of the mth node and $(Y_m^{NN})_{out}$ be the current output of the mth node network. The error variation of the network is exposed that the input components which are taken as the updated parameter of GSA. The actual outputs are tested and established on the GSA parameters are updated.

4. The recent output of the network is revealed by following,

$$(Y_{m`}^{NN})_{out} = f(Y_m) + \sum_{n=1}^{N} W_{mp} Y_m^{NN}(n) \qquad (23)$$

Where, $m = 1, 2, 3, 4$ is the bias function and $f(Y_m)$ is the mth node respectively.

$$Y_m^{NN}(n) = \frac{1}{1 + \exp(-w_{11n} Y_m - w_{111} Y_m)} \qquad (24)$$

The above equation is the activation function of output and hidden layer. The bias function of radial bias function is stated as follow,

$$f(Y_m) = \sum_{k=1}^{N} w_{mk} H_i(Y_m) \qquad (25)$$

Where, N is the number of neuron, w_{mi} be the weight of the ith neuron, $H_k(Y_m)$ are the response of the ith neuron of the hidden layer.

5. Afterward, the new weights of each neurons of the network are update by the subsequent equation.

$$w_{new} = w_{previous} + \Delta w \qquad (26)$$

Where, $\Delta w = \delta . Y_m . BP_{Error}^m$ be the change in weight, δ be the learning rate (0.2 to 0.5).

6. Repeat the above steps until the BP_{Error}^m becomes lessened.

The network is trained to deliver the target output once the training process is completed. The output for the GSA updating process has distinctive inputs. As need inputs, only respective output node affords a maximum output. So, the GSA updated process is optimally done applying the RBFNN network. The complete description of the operation consideration is explored in the section 4.

4. Results and discussion

In the part, the execution of the probable method is analyzed with the BLDC motor. In the MATLAB/Simulink platform, the probable hybrid technique-built control system has been accomplished. The motor process wants controlled under numerous circumstances to enable a positive valuation of the motor process can be achieved. Now, FOPID regulator is active to switch the speed and torque of the BLDC motor. To set the gating indications of the power adjustments only and describe the real situations in replication as adjacent as probable the electrical model of the BLDC motor. To analyze the expected system, the whole system functioning and concentrates the switch system of the suggested method is observed. The application of the suggested procedure is related with the existing methods as GSA and RBFNN methods. The Simulink diagram of the proposed system with the BLDC motor is demonstrated in the diagram 4. In this bit, the value of the proposed procedure is assessed in under section.
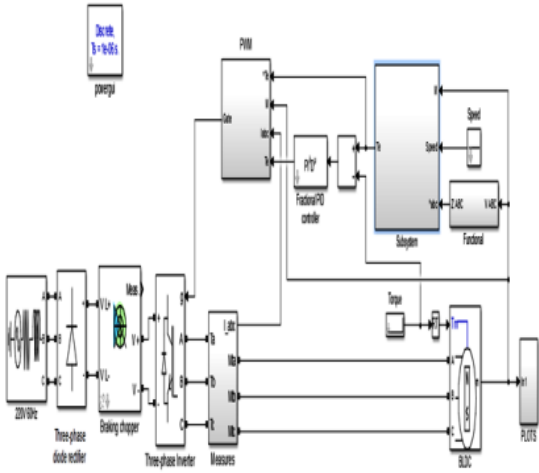
Fig.4 Simulink diagram of the BLDC motor with proposed method

Presently, the performance analysis of the suggested and current methods is scrutinized. Mainly, the orientation speed and torque graph of the BLDC motor is evaluated. Then, the BLDC motor speed, torque, current and back EMF is evaluated by several procedures. Also, the implementation parameters of the BLDC motor and suggested technique is tabulated in table 1 and 2. In the time instant t=0.2 sec, the actual speed of the motor varies the various regulator with regard to 400 rpm as the orientation speed. To evaluate the efficiency of the proposed technique is analyzed in two cases such as the reference speed in 400 rpm and 800 rpm.

➢ Case A: BLDC motor works at 400 rpm
➢ Case B: BLDC motor works at 800 rpm

These two cases are explained and the performance of suggested technique is established in the following.

Table 1: Implementation parameters of Algorithms

Descript the torque ripple reduction and **ion**	**Algorithms**	**Values**
N		10
Number of solutions		50
Maximum iteration	GSA	100
Dimension		1
Alpha		20
Gravitational constant		10
Crossover rate	GA	0.3
Mutation rate		0.2
W(min, max)	RBFNN	(0,1)
Learning rate		0.1

Table 2: Implementation parameters of BLDC motor

| S.No.	Description	Values
1.	Inertia	0.089 J(kg.m^2)
2.	Stator phase resistance (Rs)	0.2 (ohm)
3.	Flux linkage	0.175
4.	Back EMF flat area	120 (degrees)
5.	Stator phase inductance (Ls)	8.5e-3
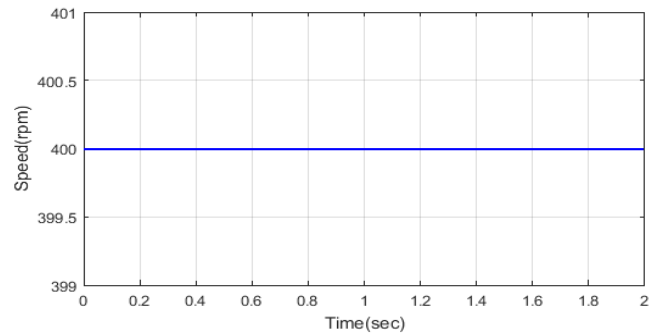
(a)
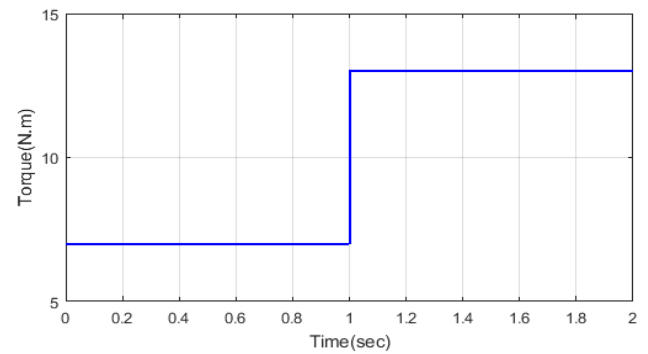
(b)

**Fig.5 Illustration of (a) Reference Speed and (b) Torque**

4.1. Analysis of Case A

The speed retort of the BLDC motor drive system amongst the suggested technique is visible in the orientation speed is about 400 rpm and the actual speed of the motor is estimated at the time of about time t= 0.2 sec. Afterward the fraction of second over the speed of the motor is reduced to the base level. Then the fluctuations in the curve have been lessened and the curve induct to achieve the stable condition at time t=0.5rad/sec. Diagram 6 (a), (b), (c), (d) and (e) depicts the vibrant retorts of the current, back EMF, speed, torque and assessment of torque error for the expected method. To prove the efficiency of the suggested scheme is equated with the existing approaches such as Genetic Algorithm (GA) and Particle Swarm Optimization (PSO) - Radial Basis Function Neural Network (RBFNN) consistently. Particular focal evidences can be

evaluated from the torque assessment error perspective of this Diagram. In the projected regulator system policy for leveling the assessed speed has been exploited as response signal in speed and torque regulators. To confirm a claim, a new procedure has been accomplished for the projected performance by launching the conditions are stated in this section. So, it can be presumed from the diagram, the projected method can be excepted where speed passing state is great status.
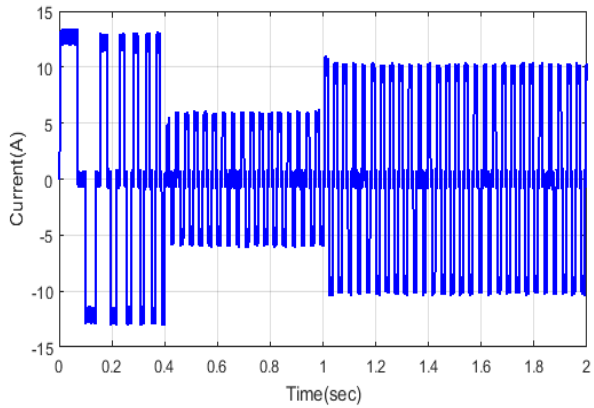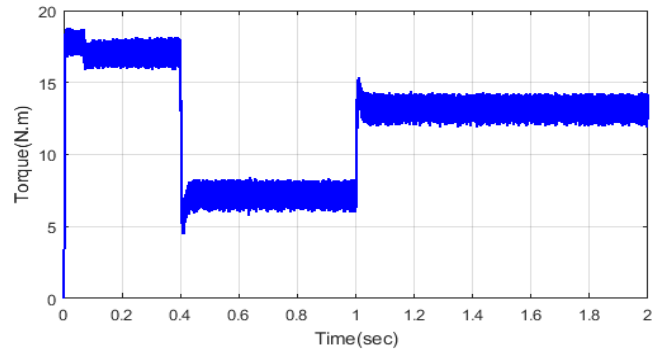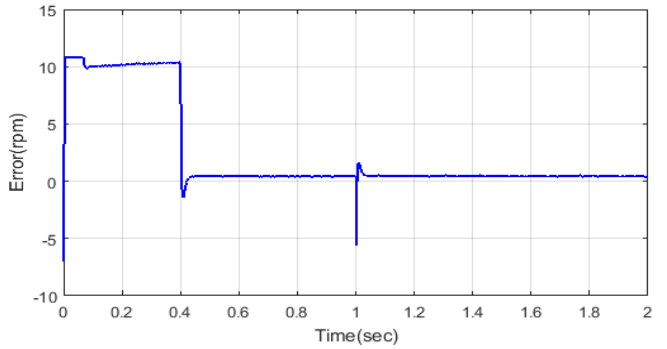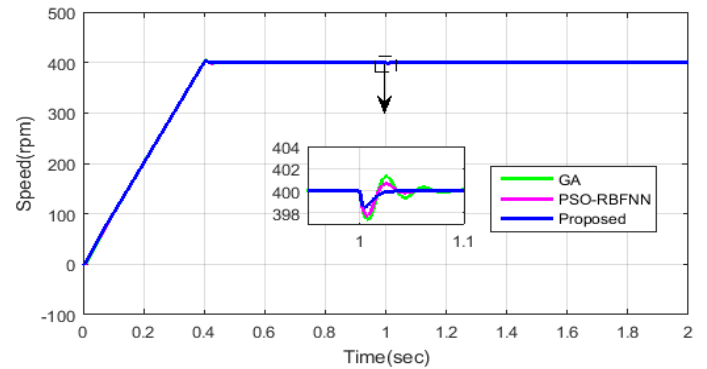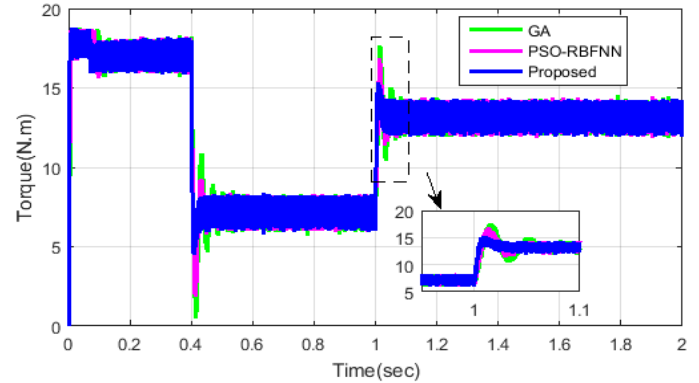

(a)
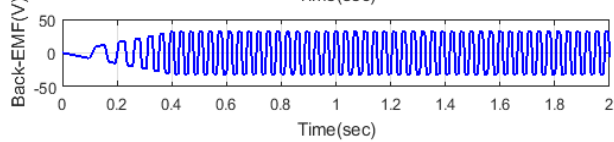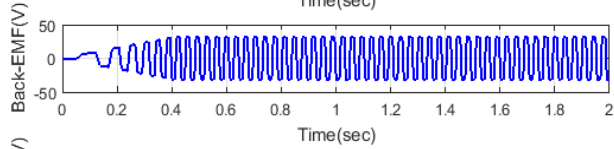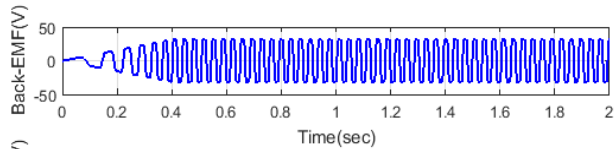
(b)
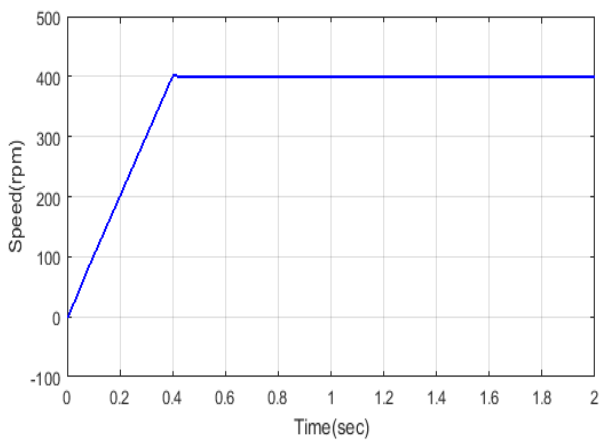
(c)

(d)

(e)

Fig.6 Illustrations of the (a) current (b) back EMF (c) Speed (d) Torque and (e) Torque error using proposed method
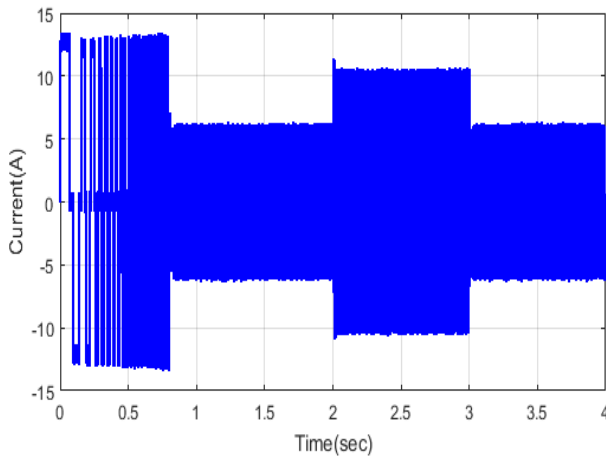

(a)

(b)

Fig. 7 Comparison analysis of (a) Speed and (b) Torque of BLDC motor in case A
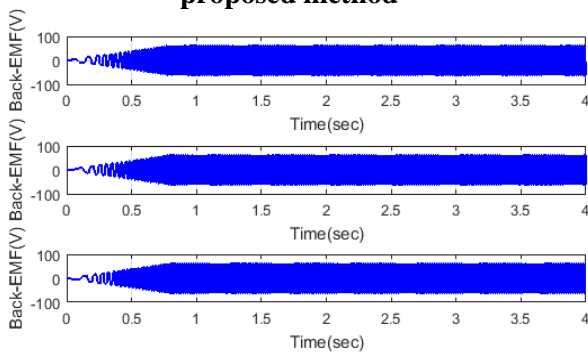
In such condition, the premise of the high-recurrence swells is seen in the figures. In the interim, commutation flows shape in inharmonic and inclined route in fast task mode, this torque swell could be insured as the engine is amplified by a present commotion at rapid, and the anticipated framework can readily. Likewise, the examination investigation is implied in the figure 7. In the diagram, the time instant t= 0 to 2sec, the torque error standards are analyzed. Now, the reduced error standards are attained about 0.03 at the time instant t= 0.5 to 0.2sec. Likewise, the case B analysis of the expected and existing methods is explicated in the following section.
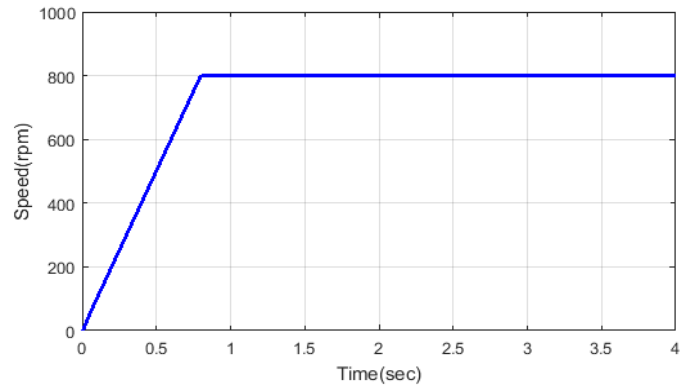
4.2. Analysis of Case B

As valued the intended method has signified efficiently in retort to high-speed operation, and the motor can endure constant process is shown in diagram 8. Now, the BLDC motor is controlled in the speed 800 rpm. Next, the torque ripples, current, speed and back EMF are assessed and established in the figure 8 and 9. The BLDC motor features are evaluated by applying the current methods. Advanced, the comparison analysis of the expected and existing methods is depicted in the following section.
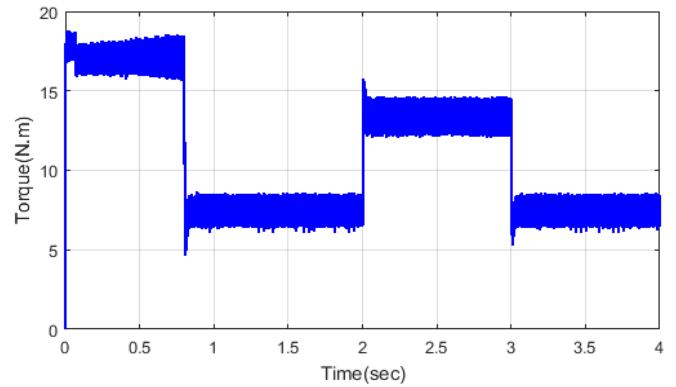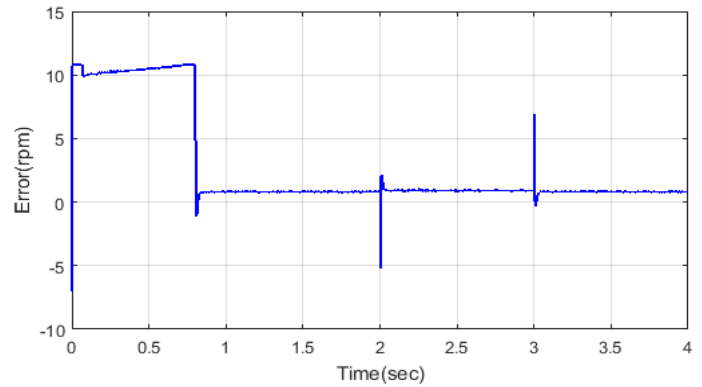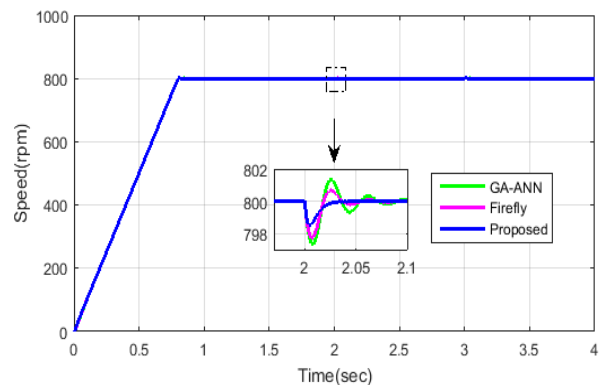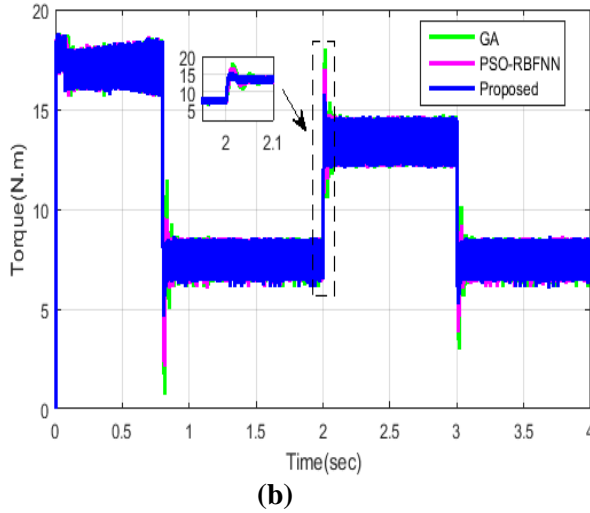
(b)

(c)

(d)

Fig.9 Analysis of (a) EMF (b) speed (c) torque and (e) Torque error using proposed method

Likewise, the comparison analysis is evaluated and applying several approaches; it is shown in the following figures.

Fig.8 Analysis of Current in BLDC motor using proposed method

(a)

(a)

(b)

Fig. 10 Comparison analysis of (a) Speed and (b) Torque of BLDC motor in case B

To conquer the torque-swell or torque plunges at rapid, the anticipated FOPID controller begins working in parallel with the anticipated technique for minimizing the substitution torque-swell. Outlines 10 (a) & (b) shows the replication results for waveforms of electromagnetic torque and speed applying of the suggested strategy to reducing replacement torque-swell at the 300 r/min correspondingly. As Fig. 10, the controller has not possessed the capacity to prevail with fast compensation current swell of the engine in substitution break without admitting the anticipated adjusting control even by controlling the DTC procedure such issue has coordinated to the development of an undesired replacement torque-swell for the engine. In this way, the torque swell can nearly drop to its half incentive by misusing the anticipated drive policy. Then, the FOPID gain impediments are overviewed and communicated applying the anticipated framework, PSO-RBFNN and GA methods is detailed in the table 3.

Table 3: Gain parameters of FOPID controller

Methods	FOPID parameters				
	K_p	K_i	K_d	λ	μ
GA	4.42	8.34	6.64	0.39	0.58
PSO-RBFNN	5.335	5.145	5.745	0.38	0.47
Proposed Method	5.542	6.824	2.425	0.53	0.386

Table 4: Under the speed variation analyzed the torque ripple reduction

Speed in rpm	Torque ripple in %		
	GA	PSO-RBFNN	GSA-RBFNN (proposed)
400	15.01	13.5	8.21
800	21.2	15.3	9.89

Currently, the suggested calculation is related to increase the torque deviation that is contrasted then GA and PSO-RBFNN as 6.81 % and 5.3%. Similarly, the speed is 800 rpm and the suggested method for GSA-RBFNN design is increased the torque deviation contrasted and alternate strategies like GA (11.4%) and PSO-RBFNN (5.5%).

As whole appraisal, the anticipated method attains preferable outcomes over uttermost techniques, as GA strategy and PSO-RBFNN methods. Instantly, more power on calculation time is on-line structure of estimator. In this worship, the anticipated framework is set up to reduce the torque swells of the BLDC motor. Contrariwise, the GA procedure and PSO-RBFNN techniques have surveyed to lessen the torque swells and propose the power over the suggested strategies from calculation trouble confinement alteration disposition. To outline, the expected control structure increases strength, accuracy of the drive framework at the expense of extra computational trouble and variable. The new additional impediments are associated to PSO-RBFNN and GA techniques.

5. Conclusion

In this article, a control approach has been accessible for scheduling a BLDC motor to the torque and speed control. By misusing the projected technique centered FOPID director is functioned for the reason of torque ripple reducing and drives presentation advancement. The projected FOPID regulator is applying the GSA and RBFNN. An established on the reproduction outcomes, the projected technique centered FOPID regulator evidences to confirm great strength, very low compassion, outstanding assessment, and condensed torque-ripple in reaction to each state conceived for evaluating the performance of the motor. Also, the FOPID regulator is modified by applying GA and PSO-RBFNN methods and observed the torque ripple, swiftness of the BLDC motor. The reproduction outcomes establish that the projected

method attained improved results once linked to additional methods. Hereafter associating to the positive procedure outcomes, the proposed regulator energy policy with its great sturdiness and exclusion of any restraint in the back-EMF energetic can assuring the energy to the motor in the direction of a constant pressure and less process in infinite high-functioning submissions in a huge speed.

Conflict of Interest

I have no conflict of interest

References

[1] Jiancheng Fang, Xinxiu Zhou and Gang Liu, "Precise Accelerated Torque Control for Small Inductance Brushless DC Motor", IEEE Transactions on Power Electronics, Vol.28, No.3, pp.1400-1412, 2013

[2] X.Z.Zhang and Y.N.Wang, "A novel position-sensor less control method for brushless DC motors", International Journal of Energy Conversion and Management, Vol.52, pp.1669–1676, 2011

[3] Sekhar P, Mohanty S., "An online power system static security assessment module using multi-layer perceptron and radial basis function network", International Journal of Electrical Power & Energy Systems, Vol. 76, pp. 165-73, 2016

[4] Salih BarisOzturk, William C.Alexander and Hamid A.Toliyat, "Direct Torque Control of Four-Switch Brushless DC Motor With Non-Sinusoidal Back EMF", IEEE Transactions on Power Electronics, Vol.25, No.2, pp.263-271, 2010

[5] Jiancheng Fang, Xinxiu Zhou and Gang Liu, "Instantaneous Torque Control of Small Inductance Brushless DC Motor", IEEE Transactions on Power Electronics, Vol.27, No.12, pp.4952-4964, 2012

[6] Jiancheng Fang, Haitao Li and Bangcheng Han, "Torque Ripple Reduction in BLDC Torque Motor With Non ideal Back EMF", IEEE Transactions on Power Electronics, Vol. 27, No.11, pp. 4630-4637, 2012

[7] Puri V, Chauhan YK, Singh N., "Parameter estimation of permanent magnet synchronous machine using Gravitational search algorithm", In proceedings of IEEE 6th International Conference on Power Systems (ICPS), pp. 1-6, 2016

[8] Yang Liu, JinZhao, MingziXia and HuiLuo, "Model Reference Adaptive Control Based Speed Control of Brushless DC Motors with Low-Resolution Hall-Effect Sensors", IEEE Transactions on Power Electronics, Vol.29, No.3, pp.1514-1522, 2014

[9] Katal N, Kumar P, Narayan S., "Optimal PID controller for coupled-tank liquid-level control system using bat algorithm", In proceedings of IEEE International Conference on Power, Control and Embedded Systems (ICPCES), pp. 1-4, 2014

[10] Sang-Young Jung, Yong-Jae Kim, Jungmoon Jae and Jaehong Kim, "Commutation Control for Low Commutation Torque Ripple in Position Sensor less Drive of Low-Voltage Brushless DC Motor", IEEE Transactions on Power Electronics, Vol.29, No.11, pp.5983-5994, 2014

[11] Jeon J, Na S, Heo H., "Cascade Sliding Mode—New Robust PID control for BLDC motor of In-wheel system", In proceedings of IEEE 10th International Conference on Environment and Electrical Engineering (EEEIC), pp. 1-4, 2011

[12] S.A.KH. Mozaffari Niapour, M.Tabarraie and M.R.Feyzi, "Design and analysis of speed-sensor less robust stochasticL1-induced observer for high-performance brushless DC motor drives with diminished torque ripple", International Journal of Energy Conversion and Management, Vol.64, pp.482–498, 2012

[13] Kun Xia, Jing Lu, Chao Bi, Yuan Tan and Bin Dong, "Dynamic Commutation Torque-Ripple Reduction for Brushless DC Motor Based on Quasi-Z-Source Net ", IET Electric Power Applications, 2016

[14] G.Scelba, G.De Donato, M.Pulvirenti, F.GiuliiCapponi and G.Scarcella, "Hall-Effect Sensor Fault Detection, Identification and Compensation in Brushless DC Drives", IEEE Transactions on Industry Applications, Vol.52, No.2, pp.1542-1554, 2016

[15] Yanhui Xu, NejilaParspour and Ulrich Vollmer, "Torque Ripple Minimization Using Online Estimation of the Stator Resistances With Consideration of Magnetic Saturation", IEEE Transactions on Industrial Electronics, Vol.61, No.9, pp.5105-5114, 2014

[16] Mehdi Salehifarn and Manuel Moreno-Equilaz, "Fault diagnosis and fault-tolerant finite control set-model predictive control of a multiphase voltage-source inverter supplying BLDC motor", ISA Transactions, Vol.60, pp.143–155, 2016

[17] Lianghui Dong, JuriJatskevich, Yingwei Huang, Mehrdad Chapariha and Jinglin Liu, "Fault Diagnosis and Signal Reconstruction of Hall Sensors in Brushless Permanent Magnet Motor Drives", IEEE Transactions on Energy Conversion, Vol.31, No.1, pp.118-131, 2016

[18] Rajan Kumar and Bhim Singh, "BLDC Motor Driven Solar PV Array Fed Water Pumping System Employing Zeta Converter", IEEE Transactions on Industry Applications, Vol.52, No.3, pp.2315-2322, 2016

[19] An-Chen Lee, Samuel Wang and Chia Juei Fan, "A Current Index Approach to Compensate Commutation Phase Error for Sensor less Brushless dc Motors with Non-ideal Back EMF", IEEE Transactions on Power Electronics, Vol.31, No.6, pp.4389-4399, 2016.